An ab Initio Study of Fructose in the Gas Phase

Alice Chung-Phillips* and Ying Ying Chen†

Department of Chemistry, Miami University, Oxford, Ohio 45056

Received: December 4, 1998

Seventy-two electronic structures of D-fructofuranose (D-FF) in the gas phase were determined by full geometry optimizations at the HF/6-31G* level. Twenty-nine structures, including the lowest energy species of nine distinct hydroxymethyl conformations of each anomer ($\alpha1-\alpha9$ and $\beta1-\beta9$), were selected for a detailed study of geometry, energy, atomic charges, and hydrogen bonding. The preferred furanose ring conformations were found to center around $^3T_2$ and $_3T^4$ for the respective α and β anomers, both of which support a quasi-axial position of the anomeric C2−O2 bond. These findings are consistent with the results from calculations on tetrahydrofuran (THF) and 2-hydroxytetrahydrofuran (2-HO-THF) at the same level. Calculated geometries are in reasonable agreement with the solid-state data on the fructose residues of di-D-fructose anhydride III, 1-kestose, and sucrose. The most stable α and β anomers at 298.15 K, α1 and β1, have the gauche−gauche (GG) orientation of the hydroxymethyl C6−O6 bond relative to the ring C5−O5 and C4−C5 bonds and a gauche−trans (GT) orientation of the hydroxymethyl C1−O1 bond relative to the ring C2−O5 and C2−C3 bonds. Effects of basis set and electron correlation on calculated energies were deduced from HF, MP2, and MP4 calculations using the 6-31G**, 6-31+G**, and 6-311++G** basis sets on two 2-HO-THF conformers and the D-FF α1 and β1 anomers. Results indicate that basis extension diminishes, whereas electron correlation enhances, hydrogen bonding. Relative electronic and Gibbs free energies of the 11 most populated α- and β-D-FF conformers at 298.15 K were estimated at the MP2/6-311++G** composite level based on HF/6-31G** geometries. This study provides physical data for parametrizing carbohydrate force fields in molecular modeling and promotes understanding of the anomeric and conformational properties of fructose structures.

Introduction

Carbohydrates play a major role in the biological processes of living organisms.[1−3] The properties of carbohydrates largely depend on their molecular structures. The two simple sugars, D-glucose and D-fructose, are of particular interest because they are components of sucrose. To date, D-glucopyranose is the most widely studied monosaccharide owing to its stable six-membered pyranose ring and prominent presence in polysaccharides.[4,5] In contrast, there is no simple stereochemical description for D-fructose. Fructose crystallizes in the β-pyranose ring form[6] but tautomerizes in aqueous solution to yield the α-pyranose, β-pyranose, α-furanose, and β-furanose ring forms.[7] Although β-furanose exists in numerous di- and oligosaccharides, relatively few crystals are found to contain the α-furanose residue.[8−10] Recent mass spectrometric measurements of gas-phase basicity (GB) showed a slim success for D-glucose but a failure for D-fructose presumably because the latter broke down more easily in the glycerol matrix.[11]

Fructose occurs in fruits and vegetables. As a sweetener, fructose is used increasingly in the Western diet because it appears to be beneficial for obese and diabetic people. Fructose is the building block of fructan polymers such as inulin and levan.[12] Other furanoses, ribose and 2-deoxyribose, are the sugar components of the nucleic acids RNA and DNA.[2] In the past decade a review of the chemical and physical properties of fructose-containing compounds,[13] an analysis of fructofuranose conformations by the molecular mechanics (MM) method,[14] and an MM3 modeling of stable conformations of the four fructose tautomers[15] contributed significantly to the understanding of this class of compounds. Quantum mechanical studies included an investigation of the relationship between sweetness and intramolecular hydrogen-bonding networks in hexuloses using the semiempirical molecular orbital (MO) method AM1,[16] several ab initio MO studies on the structures of RNA-related furanoses at the Hartree−Fock (HF) level of theory with the STO-3G, 3-21G, and 6-31G* basis sets,[17] and an examination of potential energy surfaces and compositions of D-aldo- and D-ketohexoses using the HF and density functional theory (DFT) B3LYP methods with the 6-31G** basis set.[18]

In view of the abundance and importance of fructose ($C_6H_{12}O_6$) and a general lack of experimental and theoretical data on free fructofuranose, we present here an ab initio study on the conformational properties of α- and β-D-fructofuranose in the gas phase. This is a formidable task in view of the 3^7 or 2187 possible conformations from internal rotations about the seven exocyclic bonds in each anomer. Furthermore, each exocyclic conformation can have more than one ring conformation because of pseudorotation. The objective is to find reliable electronic structures and to explain their relative stability. Specifically, the calculated geometric parameters, atomic partial charges, and relative energies may serve as useful data for parametrizing carbohydrate force fields in molecular modeling.[19,20] The favored ring shapes and hydrogen bonding patterns identified from the low-energy conformers may help us understand their influence on the relative stability of fructose-related species. More generally, a knowledge of the intrinsic property of this monosaccharide is important to the development of stereochemistry of carbohydrates.

† Current address: Department of Chemical Engineering and Material Science, Institute of Technology, University of Minnesota, Minneapolis, MN 55455.

10.1021/jp9846126 CCC: $18.00
Published on Web 01/29/1999

TABLE 1: Conformational Parameters, Ring Phase Angle (ϕ), Anomeric Parameter (D2), Ring Energy (ΔE_R), and Electronic Energy (ΔE_e) for Selected D-FF Structures at the HF/6-31G* Optimized Level[a]

		d6	d4	d3	d2	d1	ϕ	D2	ΔE_R	ΔE_e
α1	GGGT	g+	g−	g+	g+	g+	54	78	0.00	0.00
α2	GTGT	g−	g−	t	g+	g+	57	80	0.28	2.55
α3	TGGT	g−	g−	t	g+	g+	63	84	0.18	3.15
α4	GGGG	g+	g−	g+	g+	g+	75	93	0.58	−0.32
α5	GTGG	g−	g+	g−	g−	g+	61	87	0.66	2.78
α6	TGGG	t	g+	g−	g−	g−	64	89	0.36	3.12
α7	GGTG	g+	g−	g+	t	g−	59	83	0.02	1.93
α8	GTTG	g−	g+	g−	g−	g+	76	99	−0.20	2.62
α9	TGTG	t	g+	g−	g−	g+	77	100	−0.34	3.32
α1a	GGGT	g+	g−	t	g+	g+	50	75	0.44	0.77
α4a	GGGG	g+	g+	g+	g−	g+	81	102	0.72	0.79
α4b	GGGG	g−	g−	g−	g+	g−	73	91	1.01	0.93
α4*	GGGG	g+	g+	g−	g+	g+	294	111	0.12	3.54
α4a*	GGGG	g+	g+	g+	g−	g−	272	131	0.05	4.07
α8*	GTTG	g−	g+	g−	g−	g+	303	110	0.10	5.19
β1	GGGT	g+	g+	g+	g−	g−	254	−95	−0.34	0.18
β2	GTGT	g−	g+	g+	g−	g−	252	−90	−0.28	1.50
β3	TGGT	g+	g+	g+	g−	g−	265	−98	−0.30	2.21
β4	GGGG	g+	g+	g+	g−	g+	265	−99	−0.19	2.38
β5	GTGG	g−	g+	g+	g−	g+	258	−94	−0.18	2.85
β6	TGGG	g+	g+	g+	g−	g+	268	−100	−0.27	3.41
β7	GGTG	g+	g+	g+	t	g+	251	−91	−0.16	2.02
β8	GTTG	g−	g+	g+	t	g+	251	−89	−0.16	3.91
β9	TGTG	g+	g+	g+	t	g+	263	−96	−0.15	5.23
β5b	GTGG	t	t	t	g−	t	252	−90	−0.15	13.71
β7a	GGTG	g+	g+	g+	g−	g−	278	−108	−0.03	4.78
β4*	GGGG	g+	g−	g+	t	g+	114	−116	0.72	0.81
β5*	GTGG	g−	g−	t	g+	g+	82	−135	0.98	3.69
β8a*	GTTG	t	t	g−	g−	t	115	−111	0.76	11.11

[a] See text, Table S1, and Figures 1, 3−5, and S. Dihedral angles: D6≡O6−C6−C5−O5, D1≡O1−C1−C2−O5, d6≡H6−O6−C6−C5, d4≡H4−O4−C4−C3, d3≡H3−O3−C3−C2, d2≡H2−O2−C2−O5, d1≡H1−O1−C1−C2, and D2≡O2−C2−O5−C5. Hydroxymethyl conformation is described by two pairs of letters corresponding to D6 and D1. Units: ϕ and D2 in degrees; ΔE_R and ΔE_e in kcal/mol relative to E_R −230.9758240 and E_e −683.3324327 hartree of α1.

One of our continuing research objectives is to identify the theoretical levels that are at once practical and reliable for biochemical studies.[21,22] Our previous study on the GB of D-glucopyranose involved geometry optimizations at the HF/6-31G* level.[21] Although D-fructofuranose (D-FF) is structurally more complex, we proceed to examine the effects of basis set and electron correlation on the calculated structures and to find the relative distributions of different conformers. Our efforts should benefit future ab initio applications to carbohydrates.

Computational Procedure

The Gaussian 94 program was used for the ab initio calculations.[23,24] Numerous conformers of both α and β anomers of D-FF and comparable structures for the tetrahydrofuran (THF) and 2-hydroxytetrahydrofuran (2-HO-THF) were determined by full geometry optimizations at the HF/6-31G* level. Optimizations using the DFT B3LYP[25] and the second-order Møller−Plesset perturbation (MP2) methods to include electron correlation and single-point (SP) calculations with larger basis sets (e.g., 6-31G**, 6-31+G**, and 6-311++G**) were also performed on α1 and β1, two of the most stable structures of D-FF. SP calculations at the higher correlated level MP4 were carried out for 2-HO-THF. Atomic partial charges as determined by the CHELPG electrostatic fitting procedure[26] were calculated for selected structures.

TABLE 2: Properties of Tetrahydrofuran (THF) and 2-Hydroxytetrahydrofuran (2-HO-THF) at the HF/6-31G* Optimized Level[a]

	THF		2-HO-THF		
	α	exptl[b]	αg	αt	αg*
geometrical parameters[c]					
C−H	1.085	1.096	1.083	1.084	1.084
O−H	−	−	0.949	0.947	0.946
C−C	1.528	1.536	1.529	1.531	1.528
C5−O5	1.409	1.428	1.418	1.416	1.411
C2−O5	1.409	1.428	1.390	1.377	1.402
C2−O2	−	−	1.393	1.400	1.380
C2−O5−C5	111.3	110.5	110.8	111.1	112.1
O2−C2−O5	−	−	111.3	108.2	110.4
O2−C2−O5−C5 (D2)	−	−	90.0	90.3	136.3
H9−O2−C2−O5 (d2)	−	−	52.0	169.1	−47.2
O5−C5−C4−C3 (φ1)	30.4	29.6	18.2	17.4	−29.8
C2−O5−C5−C4 (φ2)	−12.0	−11.6	5.3	7.0	11.7
C3−C2−O5−C5 (φ3)	−12.0	−11.6	−27.0	−28.9	11.7
C4−C3−C2−O5 (φ4)	30.4	29.6	37.0	38.2	−30.1
C5−C4−C3−C2 (φ5)	−36.0	−35.0	−32.5	−32.6	35.6
ϕ	90	90	67	65	270
q	0.37	0.38	0.36	0.37	0.36
symbol	^3_4T	^3_4T	$^3T_2$	$^3T_2$	^4_3T
rotational constants and dipole moment[d]					
A	7191	7099	5619	5625	6836
B	7105	6976	3826	3806	3347
C	4053	4008	3001	3009	2510
μ	1.94	1.75	0.79	2.77	2.88

[a] See Figure 2 and Tables S3 and S4. Atom numbering conforms to D-FF in Figure 1. E_e (hartree): THF −230.9764463; 2-HO-THF g −305.8441570, t −305.8373866, and g* −305.8393890. [b] Reference 31. [c] Bond length A−B in Å; bond angle A−B−C and dihedral angle A−B−C−D in degrees. Mean values for C−H and C−C are listed. The ring parameters are ϕ in degrees for phase, q for puckering, and a symbol for the ring shape. [d] Rotational constants A, B, and C in MHz; μ in debye (D).

Electronic energies (E_e) of the 11 most stable D-FF structures were improved by reoptimizations at the HF/6-31G** level, followed by HF/6-311++G** and MP2/6-31G** calculations at the HF/6-31G** geometries. Results were used to deduce E_e at the composite level "MP2/6-311++G**". (This procedure is analogous to the G1 and G2 theories of Pople and coworkers.[27]) The same composite level, but evaluated at a better geometry (MP2/6-31+G**), was applied to α1 and β1 for comparison. Harmonic vibrational frequency calculations were carried out at the HF/6-31G* optimized level for all 11 structures to obtain zero-point energy E_{ZP}, internal energy change ($E - E_0$), and entropy S for estimating the thermal contribution to Gibbs free energy G at 298.15 K, G_{therm}.[22a] Here, the E_{ZP} was scaled by a factor of 0.9135.[28]

The option SCF = TIGHT was used in all SP calculations. The frozen-core approximation was employed in MP2 and MP4 applications. The MP2/6-31+G** optimizations on α1 and β1 were the largest calculations which took 40 CPU h on a Cray T90 supercomputer.

Results and Discussion

Extensive searches for the α- and β-D-FF conformers that might help identify the physical factors responsible for their relative stability led to 72 structures (Table S1), from which 29 (Table 1) were selected for systematic evaluations. Areas of investigation include THF and 2-HO-THF as model compounds, conformational analysis of D-FF, effects of basis set and electron correlation on calculated structures, and equilibrium distribution of gaseous D-FF. Results are presented in Tables 1−7 and Figures 1−5, supplemented by Tables S1−S8, Figure S, and

TABLE 3: The H−Bonds (*i*H*k*) and Their Distances [*r*(*i*H*k*)] in Selected D-FF Structures at the HF/6-31G* Optimized Level[a]

		1*H*5	6*H*5 (2*H*4)[b]	4*H*2 (3*H*1)	1*H*3 (1*H*2)	2*H*1 (6*H*3)	3*H*6 (1*H*6)	6*H*1
α1	GGGT	2.53	2.55	2.17		2.25	2.05	
α2	GTGT	2.55	2.39	2.19		2.26		
α3	TGGT	2.51		2.16		2.23		
α4	GGGG		2.40	2.23	2.17		1.94	2.42
α5	GTGG	2.47	2.40	(2.11)[b]	(1.97)			
α6	TGGG	2.41		(2.08)	(1.98)			
α7	GGTG		2.55	2.21		2.34	2.03	
α8	GTTG		2.37	(2.25)	(2.46)	(2.53)		
α9	TGTG			(2.23)	(2.45)	(2.52)		
α1a	GGGT	2.53	2.51	2.21		2.25	(2.41)	
α4a	GGGG		2.42	(2.29)	2.21		1.91	2.26
α4b	GGGG	2.39		2.21	(1.98)		(2.04)	2.26
α4*	GGGG		2.40		2.31			2.59
α4a*	GGGG		2.56		(2.18)			(2.16)
α8*	GTTG		2.45		(2.11)	(2.32)		
		1*H*5	6*H*5 (2*H*3)	3*H*2 (4*H*1)	1*H*3 (1*H*2)	2*H*1 (3*H*6)	6*H*4	6*H*2
β1	GGGT	2.56	2.45	2.21		2.21		2.55
β2	GTGT	2.56	2.45	2.20		2.26		
β3	TGGT	2.51		2.17		2.27	2.43	
β4	GGGG	2.38	2.45	2.19				
β5	GTGG	2.39	2.45	2.20				
β6	TGGG	2.41		2.18			2.40	
β7	GGTG		2.46	2.29	2.57	2.20		2.41
β8	GTTG		2.43	2.25	2.57	2.25		
β9	TGTG			2.20	2.60	2.32	2.44	
β7a	GGTG		2.45	2.17		(2.46)		
β4*	GGGG	2.51	2.50	(1.98)	(2.07)		(1.98)	2.42
β5*	GTGG	2.50	2.34	(2.02)	(1.99)			

[a] See Table 1. *i*H*k* is O*i*—H*j*···O*k* and *r*(*i*H*k*) is the H···O distance listed in Å. [b] Value in parentheses follows the heading in parentheses. β5b, GTGG, has none. β8a*, GTTG, has only 2*H*3 at 2.03 Å.

TABLE 4: Geometrical Parameters, Dipole Moment, and Atomic Partial Charges in Selected D-FF Structures at the HF/6-31G* Optimized Level: Comparison with 2-HO-THF Conformers[a]

	α3 (αg)	α7 (αt)	α4a* (αg*)	β2 (βg)	β7 (βt)	β5* (βg*)
			geometrical parameters			
C2−O5	1.398	1.386	1.412	1.398	1.383	1.410
C2−O2	1.395	1.404	1.382	1.392	1.403	1.370
C2−O5−C5	110.8	110.9	113.6	110.2	112.2	113.5
O2−C2−O5	110.2	108.1	109.4	111.6	109.9	111.2
D2	83.8	83.4	131.1	−90.0	−91.4	-135.3
d2	72.9	159.2	−47.3	−79.1	−130.9	82.3
ϕ	63	59	272	252	251	82
q	0.38	0.37	0.31	0.37	0.38	0.29
symbol	$^3T_2$	^3_2T	^4_3T	$_3E$	$_3E$	$^3T_4$
			dipole moment			
μ	0.88	1.76	2.48	1.59	1.82	2.54
			atomic partial charges[b]			
O5	−0.58	−0.58	−0.59	−0.52	−0.58	−0.51
O1	−0.70	−0.71	−0.73	−0.68	−0.72	−0.66
O6	−0.72	−0.63	−0.68	−0.72	−0.72	−0.71
O3	−0.74	−0.69	−0.71	−0.73	−0.70	−0.77
O4	−0.76	−0.72	−0.75	−0.77	−0.76	−0.75
O2	−0.76	−0.66	−0.75	−0.67	−0.71	−0.81
H8 (O1)	0.43	0.45	0.41	0.44	0.43	0.42
H12 (O6)	0.43	0.43	0.44	0.43	0.45	0.42
H10 (O3)	0.47	0.39	0.43	0.45	0.41	0.48
H11 (O4)	0.47	0.43	0.46	0.47	0.46	0.43
H9 (O2)	0.48	0.41	0.46	0.47	0.46	0.53

[a] The 2-HO-THF conformer to be compared with is listed below the D-FF structure in parentheses. See Tables 2 and S3. [b] Charges (CHELPG) in e (ref 26). The D-FF charges may be compared with the HF/6-31G* charges of reference compounds below. Ether-type O: dimethyl ether −0.42; THF −0.52; and 2-HO-THF [−0.49, −0.56]. Alcohol-type O*i*, H*j* (O*i*): ethanol −0.73, 0.42; isopropyl alcohol −0.76, 0.42; *tert*-butyl alcohol −0.79, 0.42; 2-HO-THF [−0.66, −0.76], [0.40, 0.45]; and 1,2-ethanediol [−0.66, −0.76], [0.41, 0.46].

Appendix S in Supporting Information. In the following discussion all calculated values refer to the HF/6-31G* optimized level unless stated otherwise.

Conformational Nomenclature. We use α1 and β1 in Figure 1, drawn in the standard orientation for a ketofuranose ring,[14] to illustrate the nomenclature for D-FF conformation. Internal

TABLE 5: Geometric Parameters and Ring Conformations in Selected D-FF Structures at the HF/6-31G* Optimized Level: Comparison with Experiments

		α1−α9		β1−β9		β
parameter[a]	number[b]	mean	dev	mean	dev	exptl[c]
C−H	63	1.083	0.002	1.084	0.002	1.095
O−H	45	0.950	0.002	0.949	0.001	0.973
C−C exocyclic	18	1.519	0.002	1.518	0.002	1.519
ring	27	1.535	0.007	1.526	0.003	1.530
Ci−Oi i = 1, 3, 4, 6	36	1.402	0.006	1.396	0.003	1.417
C5−O5	9	1.422	0.003	1.427	0.004	1.445
C2−O5	9	1.397	0.006	1.394	0.005	1.408
C2−O2	9	1.393	0.007	1.396	0.003	1.429
C3−C2−O5	9	104.3	1.0	104.4	0.3	105.2
C4−C3−C2	9	100.9	0.3	101.4	0.4	102.3
C5−C4−C3	9	102.9	0.3	102.0	0.3	102.3
C4−C3−C2−O5	9	37.6	3.7	−35.3	1.4	−31.2
C5−C4−C3−C2	9	−32.7	1.2	36.6	1.7	35.0

	α* (GTTG)		β* (GTTG)		β (GTGG)		β (GGTG)	
ring	A1[d]	α8*	K1[e]	β8a*	K2[f]	β5	SF[c]	β7a
φ1	−36.3	−37.3	28.0	34.0	−25.8	−24.8	-27.3	−32.2
φ2	18.6	31.6	−15.2	−25.4	0.6	2.8	8.1	16.7
φ3	7.2	−11.9	−3.7	6.0	24.9	20.6	14.7	6.2
φ4	−29.4	−12.6	21.1	15.9	−40.7	-35.2	-31.2	-26.1
φ5	40.0	30.1	−29.3	−29.8	40.1	35.9	35.0	35.0
ϕ	277	303	101	115	254	258	265	278
q	0.40	0.36	0.30	0.33	0.42	0.37	0.35	0.36
symbol	$^4T_3$	^4_5T	$_4T^3$	$_4T^5$	$_3E$	$_3E$	$_3T^4$	$^4T_3$

[a] Each structure has seven C−H, five O−H, five C−C, and seven C−O bonds. [b] Total number from the nine conformers used in averaging. dev ≡ mean absolute deviation. [c] The β-D-FF (GGTG) residue of sucrose in ref 10. [d] Residue 1 of di-D-FF anhydride III in ref 8. [e] Residue 1 of 1-kestose in ref 9. [f] Residue 2 of 1-kestose in ref 9.

TABLE 6: Electronic Energies for the 2-HO-THF αg and αg* Conformers and D-FF α1 and β1 Anomers at Different Levels[a]

level: L2//L1		E_e	ΔE_e
L2 (energy)	L1 (geometry)	αg	αg*
HF/6-31G*	HF/6-31G*	−305.8441570	2.99
HF/6-31+G**		−305.8697221	2.97
HF/6-311++G**		−305.9350029	3.01
HF/6-31G*	MP2/6-31G*	−305.8409731	2.97
MP2/6-31G*		−306.7160449	3.52
MP4/6-31G*		−306.7907319	3.30
HF/6-31+G**	MP2/6-31+G**	−305.8669117	3.00
MP2/6-31+G**		−306.8046664	3.63
MP4/6-31+G**		−306.8848372	3.45

L2 (energy)	L1 (geometry)	α1	β1
HF/6-31G*	HF/6-31G*	−683.3324327	0.18
HF/6-31G**	HF/6-31G** (*i*)	−683.3758412	0.01
HF/6-311++G**	(*j*)	−683.5572816	−1.22
MP2/6-31G**	(*k*)	−685.2912595	2.40
HF/6-31+G**	HF/6-31+G**	−683.3980541	−0.94
HF/6-311++G**	HF/6-311++G**	−683.5576414	−1.26
MP2/6-31G*	MP2/6-31G* (*l*)	−685.1862699	2.67
MP2/6-31G**	MP2/6-31G** (*m*)	−685.2989271	2.44
MP2/6-31+G**	MP2/6-31+G** (*n*)	−685.3527750	0.96
HF/6-31+G**	(*o*)	−683.3893645	−0.94
HF/6-311++G**	(*p*)	−683.5480023	−1.11
"MP2/6-311++G**"	HF/6-31G** (*y*)	−685.4726999	1.16
"MP2/6-311++G**"	MP2/6-31+G** (*z*)	−685.5114128	0.79

[a] Units: E_e in hartree; and ΔE_e in kcal/mol for αg* relative to αg or β1 relative to α1 at the same level. Blank space for L1 implies "same as above".

H-bonds are highlighted by dotted lines. Calculated geometries and physical properties are provided in Tables 1, S1, and S2.

The D-FF molecule has a five-membered ring containing the O5, C2, C3, C4, and C5 atoms with two hydroxymethyl chains at C2 and C5 and three hydroxyl groups at C2, C3, and C4. The C6−O6 chain and the O3−H group lie above the ring, whereas the O4−H group lies below. The two anomers of D-FF are distinguished by the positions of the two substituents at the anomeric C2 atom: the α anomer has the C1−O1 chain above and the O2−H group below the ring, whereas the β anomer has the opposite arrangement. The α1 and β1 structures illustrate the configurational differences.

Each hydroxymethyl chain assumes three distinct orientations relative to the ring, resulting in nine conformations for each anomer. The hydroxymethyl conformations are named in analogy to those of D-glucopyranose (D-GP),[29] i.e., using the descriptors GG (gauche−gauche), GT (gauche−trans), and TG (trans−gauche) to specify the orientation of the C6−O6 bond relative to C5−O5 and C4−C5 bonds first and that of C1−O1 relative to C2−O5 and C2−C3 next. In addition, each hydroxyl Oi−H may assume one of the three staggered conformations; its dihedral angle di is described as gauche clockwise (g+), gauche counterclockwise (g−), and trans (t). Analogous notations G+, G−, and T are used for the dihedral angle Di referring to the Ci−Oi bond.

The ring conformation is described by the dihedral angles of ring atoms (φi of Table 2). The nonplanarity of the ring is characterized by the phase angle ϕ and puckering amplitude q introduced by Cremer and Pople.[30] Using ϕ, we can locate a ring symbol from a conformational wheel designed for the ketofuranoses,[14] for which the (ϕ, symbol) notations are (90°, ^3_4T) for the southmost and (270°, ^4_3T) for the northmost positions. The calculated data lead to (54°, ^3_2T) for α1, a twisted form with C3 up and C2 down about equally from the C4−C5−O5 plane, and (256°, $_3E$) for β1, an envelope form with C3 down from the C4−C5−O5−C2 plane.

The dihedral angle O2−C2−O5−C5 (D2) may supply valuable clues to the consequential anomeric effect. The D-FF ring shapes result in 78° and −95° for the D2 of α1 and β1, respectively, which are quite different from the corresponding

TABLE 7: Electronic Energies (ΔE_e), Gibbs Free Energy (ΔG), and Equilibrium Population (pop) Estimated at 298.15 K and 1 Atm for Low-Energy D-FF Structures[a]

		ΔE_e			ΔG_{therm}	"MP2/6-311++G**"		
		HF/6-31G**	HF/6-311++G**	MP2/6-31G**	HF/6-31G*	ΔE_e	ΔG	pop
α1	GGGT	0.00	0.00	0.00	0.00	0.00	0.00	28
α4	GGGG	−0.19	1.18	−1.79	0.89	−0.42	0.47	13
α4a	GGGG	0.91	2.39	−0.78	1.00	0.69	1.70	2
α4b	GGGG	0.98	2.24	−0.27	0.45	0.98	1.43	3
β4*	GGGG	0.90	2.36	−1.53	0.76	−0.07	0.69	9
α1a	GGGT	0.72	0.45	1.49	−0.46	1.22	0.76	8
α7	GGTG	1.92	1.90	2.05	−0.32	2.02	1.70	2
β1	GGGT	0.01	−1.22	2.40	−1.23	1.17	−0.06	31
β2	GTGT	1.37	−0.68	4.93	−1.55	2.88	1.33	3
β3	GTTG	2.11	0.65	5.53	−1.43	4.08	2.64	0
β7	GGTG	1.88	1.08	3.88	−1.11	3.08	1.97	1

[a] All quantities relative to those of α1. See text and Tables 6 and Table S6. $G_{therm}(\alpha 1) = 100.453$ kcal/mol. Units: ΔE_e and ΔG_{therm} in kcal/mol; pop in %.

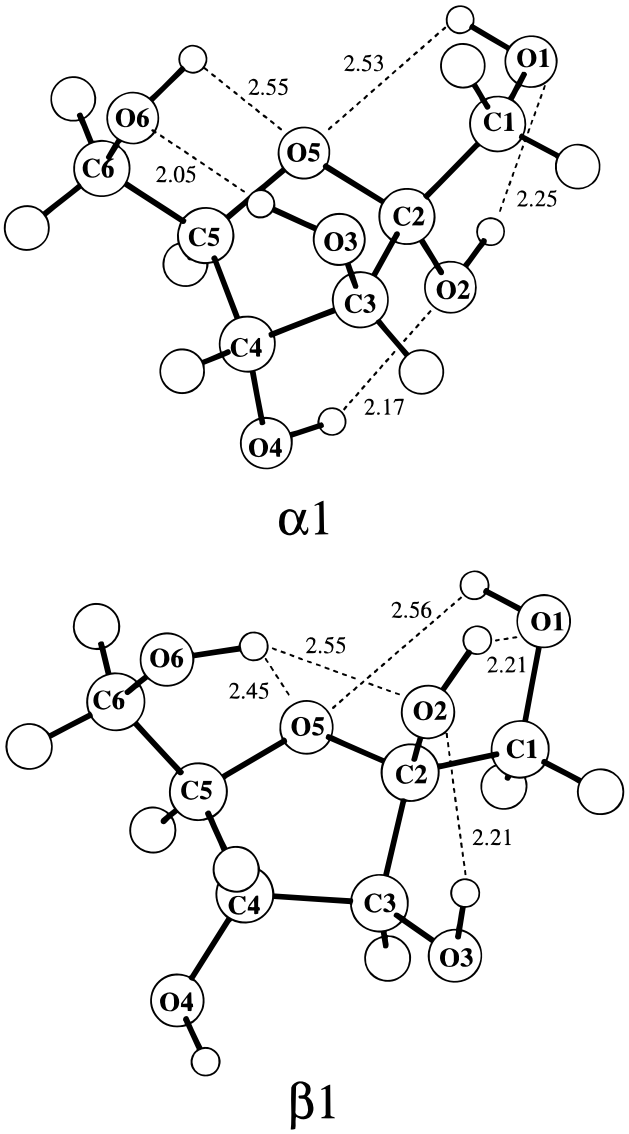

Figure 1. Two GGGT structures of α- and β-D-fructofuranose (α1 and β1). Carbon and oxygen atoms are identified with atom labels. Hydrogen atoms are numbered in a clockwise direction first for those bonded to carbons and next for those bonded to oxygens. Numbering begins at C1−C6 for H1−H7 and at O1−O4 and O6 for H8−H12. Some important H-bond distances calculated at the HF/6-31G* optimized level are shown in Å.

O1−C1−O5−C5 angle at 63° and −179° calculated for the lowest energy conformers of α- and β-D-GP.[21] In other words,

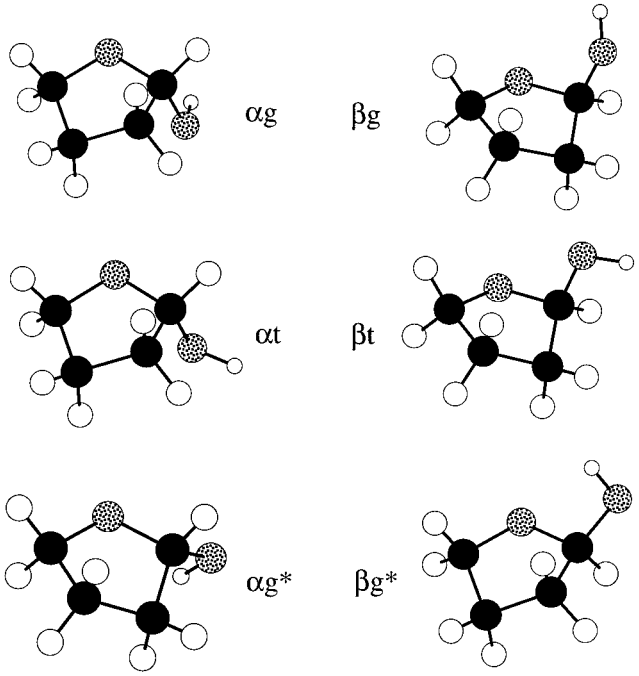

Figure 2. HF/6-31G* structures for the g, t, and g* conformers of 2-hydroxytetrahydrofuran.

the C2−O2 bond in a furanose ring no longer holds the "truly" axial (ca. 60°) and equatorial (ca. 180°) orientations of the C1−O1 bond in a pyranose ring. Most low-energy conformers of α- and β-D-FF adopt a "quasi"-axial (ca. ±90°) orientation[1] which no longer distinguishes α to be a more stable anomer than β as in D-GP.

Model Compounds. To gain an understanding of the physical factors that influence the furanose ring conformation, it is advantageous to examine furanoid structures that contain a minimal number of substituents. The choices are obviously THF, one with the ring only, and 2-HO-THF, one with a single hydroxyl at the anomeric carbon. For comparison with the α,β ring shapes of D-FF, the stable 2-HO-THF conformations are cast in the compatible α,β shapes in Figure 2. Note that each α,β pair in the same row are enantiomers of equal energy. The analogous α,β pair of THF may be visualized by replacing the OH group in the top row with a H atom.

In searching for the global minimum of the each model compound, we used a planar ring to initiate the optimization. Invariably the final α and β ring conformations reached ${}^{3}_{4}T$ and ${}^{4}_{3}T$ for THF and ${}^{3}T_{2}$ and ${}_{3}T^{2}$ for 2-HO-THF, both of which have

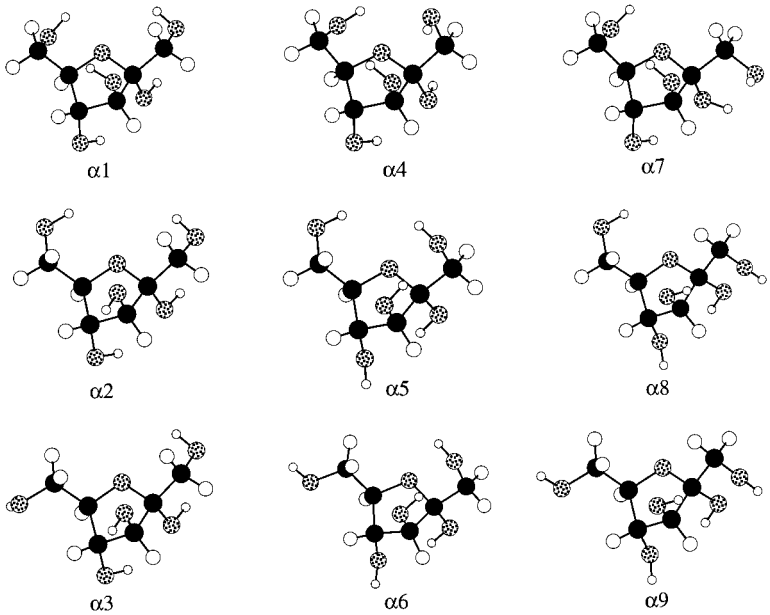

Figure 3. HF/6-31G* structures for the α1−α9 conformers of α-D-fructofuranose.

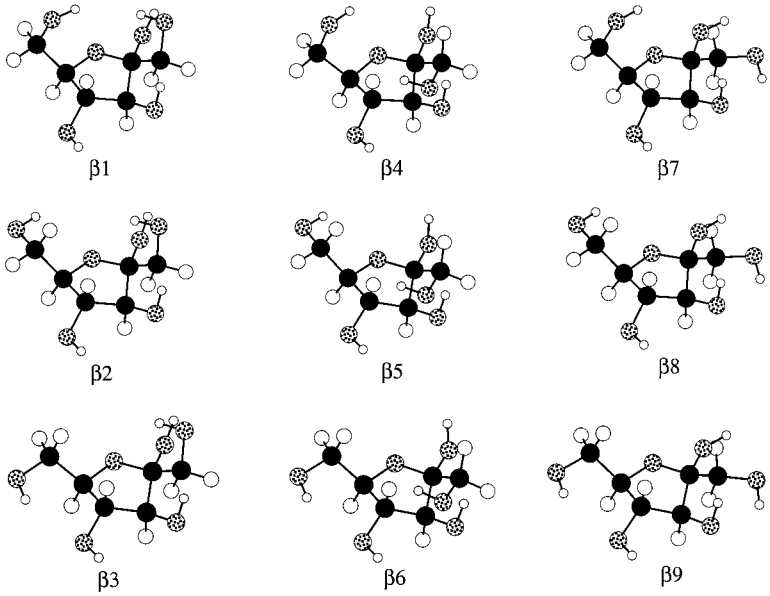

Figure 4. HF/6-31G* structures for the β1−β9 conformers of β-D-fructofuranose.

twisted ring shapes with C3 up for α and C3 down for β (top row of Figure 2). This similarity extends to D-FF with ${}^{3}_{2}T$ for α1 and ${}_{3}E$ for β1, where each structure contains five substituents and a network of five H-bonds. In other words, the favored ring shapes are not much changed by the addition of substituents on going from THF, 2-HO-THF, to D-FF.

Using the same atom numbering scheme as D-FF, we show average bond lengths and geometrical parameters pertaining to the anomeric effect and ring conformation in the model compounds for the α anomeric forms in Table 2; those for the β anomeric forms are unchanged except for a sign change on each dihedral angle. The calculated data for THF are compared with existing experimental data. Despite a discrepancy of 0.01−0.02 Å in bond lengths, bond and ring dihedral angles are within 1° of the electron diffraction values, and rotational constants and dipole moment are within 130 MHz and 0.2 D of the microwave values.[31] The good agreement suggests that HF/6-31G* yields reasonable geometry and electron distribution. In the interest of providing useful parameters for molecular modeling,[20] more complete listings including atomic partial charges and higher level results are tabulated in Tables S3 and S4.

THF has no substituent, so the global minimum must attain a ring conformation with minimal mutual repulsion among the five bonds of the furanose ring. The driving force is the ring strain. The most stable ring conformation, ${}^{3}_{4}T$ for THF α, is consistent with the knowledge that repulsion from two eclipsing bonds is greater for C−C vs C−C than for C−O vs C−C. Therefore, the puckering of the ring occurs at C3 or C4, or both, and the planar portion of the ring contains the two C−O bonds. It is of interest to have a measure of ring strain among different furanoids. To do so, we introduce the term ΔE_R as the relative ring energy between two THF-like structures *xr* and *yr* extracted from the optimized substituted-THF structures *x* and *y*. (See Appendix S.) The ΔE_R values for THF α, 2-HO-THF αg, and D-FF α1 are found to be 0.0, 0.6, and 1.9 kcal/mol, respectively, indicating that substituents increase ring strain.

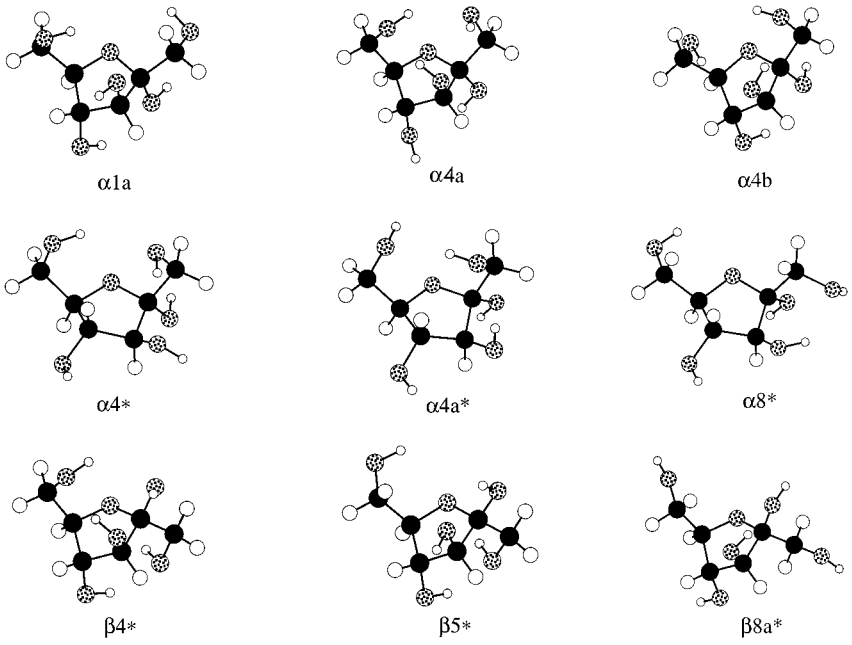

Figure 5. HF/6-31G* structures for the α1a, α4a, α4b, α4*, α4a*, α8*, *β*4*, *β*5*, and *β*8a* conformers of α- and *β*-D-fructofuranose.

The lowest energy conformer of 2-HO-THF, αg, has the OH group gauche to the C2−O5 bond. This is shown as 52° (g+) for the dihedral angle H9−O2−C2−O5 (d2). Internal rotation around the C2−O2 bond in one direction leads to the stable trans conformer αt with d2 = 169° (t), roughly keeping the same ring shape as αg ($^3T_2$). Internal rotation in the other direction brings H9 close to the H atom bonded to C4 below the ring. The steric repulsion between the two H atoms in close proximity (O2−H···H−C4) causes a pseudorotation to ^4_3T at the energy minimum d2 = −47° (g−), which is designated as αg* with the asterisk indicating a different ring shape. Applying the same procedure to *β*g ($_3T^2$) leads to *β*t ($_3T^2$) and *β*g* (^3_4T).

To simplify subsequent discussion on D-FF conformations, the four distinct conformations drawn in Figure 2 are called the α, α*, *β*, and *β** forms. The α and *β* forms have quasi-axial C2−O2 bonds (D2 ca. ±90°) and the α* and *β** forms have quasi-equatorial C2−O2 bonds (D2 ca. ±136°). The α and *β** forms have southern (S) type ring conformation ($^3T_2$ and ^3_4T) and the *β* and α* forms have northern (N) type ring conformation ($_3T^2$ and ^4_3T).

The anomeric effects that exist in the α and *β* anomers of D-GP in the $^4C_1$ chair form have been rationalized successfully by a hyperconjugation model.[32,33] In this model the highly electronegative oxygen atom O2 or O5 withdraws electrons from the carbon atom C2 through the *σ* bond orbital and back-donates electrons by delocalizing a lone-pair (lp) into the adjacent *σ** antibonding orbital. The same explanation may be applied to the 2-HO-THF αg, αt, and αg*. In the αt conformation the lp on O5 that is anti-periplanar with the C2−O2 bond undergoes an n−*σ** delocalization to effect a lengthening of the C2−O2 bond (1.40 Å) relative to the C2−O5 bond (1.38 Å); this is the endo-anomeric stabilization (endo-AS). In the αg* conformation the O2 lp anti-periplanar with the C2−O5 bond delocalizes into the *σ** orbital of C2−O5 to cause a lengthening of the C2−O5 bond (1.40 Å) relative to the C2−O2 bond (1.38 Å); this is the exo-anomeric stabilization (exo-AS). In the αg conformation, both endo-AS and exo-AS are in operation and the opposing forces roughly equilibrate the bond lengths of C2−O2 and C2−O5 (both 1.39 Å).

Some insight may be gained by reviewing the work of Salzner and Schleyer on 2-hydroxytetrahydropyran (2-HO-THP) where the geometry of the pyranose ring is more clear-cut for the hyperconjugation model.[34] The HF/6-31G* relative energies of the six 2-HO-THP conformers at the respective g+, t, and g− orientations of the O1−H bond against the C1−O5 bond were shown to be $5a_1$ 0.0, $5a_2$ 4.1, and $5a_3$ 4.1 kcal/mol for the axial (α) form and $5e_1$ 1.3, $5e_2$ 6.1, and $5e_3$ 2.0 kcal/mol for the equatorial (*β*) form.[34] A geometric analysis using molecular models reveals that $5a_1$, $5a_2$, and $5e_3$ may be matched to αg, αt, and αg*, respectively, whereas $5a_3$, $5e_1$, and $5e_2$ have no stable counterparts in 2-HO-THF. Note the geometric correspondence between a *β* conformer of 2-HO-THP, $5e_3$, and an α conformer of 2-HO-THF, αg*, showing how the well-defined α and *β* conformations in a pyranose ring no longer carry over to a furanose ring. Extending this observation to D-FF, the presence of α* form in the predominately *β* (N) region and the presence of *β** form in the predominately α (S) region of the conformational wheel is anticipated.

The two lone pairs on each oxygen atom (O2 or O5) in 2-HO-THF may be visualized to result in a dipole vector pointing along the bisectrix of the angle between the pairs. The interaction between the two dipole vectors, one from each oxygen atom, is largely responsible for the electrostatic repulsion (ER) and dipole moment (*μ*). The magnitude of interaction depends on the separation, lengths, and directions of the two vectors. The αg conformer is expected to have smaller ER and *μ* than αt and αg* because its two dipole vectors are much more opposed in their directions. The expectation is consistent with the calculated *μ* for 2-HO-THF (αg 0.79, αt 2.77, and αg* 2.88 D), which also compare well with the calculated *μ* for 2-HO-THP conformers ($5a_1$ 0.39, $5a_2$ 2.40, and $5e_3$ 2.49 D).[34] The larger *μ* (by ca. 0.4 D) is caused by a smaller dipole−dipole separation in a quasi-axial or -equatorial hydroxyl conformation compared with the truly axial or equatorial hydroxyl conformation.

The anomeric effects in two axial conformers of 2-HO-THP were analyzed recently[33] by means of natural bond orbitals (NBOs).[35] The energy of a conformer is partitioned into two major terms, hyperconjugation and Lewis. Hyperconjugation consists of the delocalization of lp on each oxygen atom into the adjacent *σ** bonds connecting the nearest anomeric carbon atom to the next-nearest oxygen, hydrogen, and carbon atoms.[33]

The Lewis energy is the energy of the molecule in the absence of hyperconjugation that includes the steric and electrostatic effects.[34] An NBO analysis on 2-HO-THF conformers would be worthwhile for comparison.

Hydroxymethyl Conformers. We have shown how ring strain, steric repulsion, and anomeric stabilization play the primary roles in determining the ring shapes of THF and 2-HO-THF, and to a large extent, the more complex D-FF structure. We next examine how interactions of different substituents in D-FF, especially those associated with hydrogen bonding, influence the charge distribution and stability of D-FF.

In Table S1 the conformational dihedral angles, E_e, and energy relative to α1 (ΔE_e) are provided for the 72 D-FF structures. The lowest energy structures of the nine hydroxymethyl conformations in the α and β forms are designated as α1−α9 and β1−β9; those of the same hydroxymethyl conformation but with increasing energy are noted by a letter, e.g., α3 is followed by α3a−α3f. Those in the α* and β* forms are differentiated with an asterisk, e.g., α3f is followed by α3*−α3b*. The conformers selected for discussion are presented in Table 1, which include the lowest energy structures of α,β forms (α1−α9, α1a, α4a, α4b, and β1−β9) and α*,β* forms (α4* and β4*), representatives of the α*,β* forms (α4a* and β5*), those for comparison with experiments (α8*, β8a*, and β7a), and one with the unique feature of having no discernible H-bonds (β5d). The exocylic conformational parameters, ring phase angle ϕ, dihedral angle D2, relative ring energy ΔE_R, and ΔE_e are provided.

To show variations of D-FF ring conformation and their relations with THF, 2-HO-THF, and experimental values, the selected structures (characterized by ring parameters φ1−φ5, ϕ, q, and symbol) are arranged in Table S5 in order of increasing ϕ for the α and β anomers separately. The D-FF values for ϕ (°) in Table 1 plus the additional five αi* and three βi* in Table S1 show αi [50, 81], αi* [272, 328], βi [251, 278], and βi* [82, 135], where [a, b] represents a range from a to b. The midpoint is about 66° ($^3T_2$) for αi and 265° ($_3T^4$) for βi. The α, α*, β, and β* forms of D-FF in Figures 3−5 and S are compatible with those of 2-HO-THF in Figure 2. Again, αi and βi* are the S conformers and βi and αi* are the N conformers. With some notable exceptions, energies of αi and βi are lower than their counterparts αi* and βi* of the same hydroxymethyl conformation as a result of a full vs partial anomeric stabilization (vide supra).

The anomeric parameter D2 varies over ranges [75°, 131°] for the α,α* forms and [−89°, −135°] for the β,β* forms, which may be compared to ±90° and ±136° of the axial and equatorial 2-HO-THF. A sensitive indicator of relative ring stability is ΔE_R, the ring energy of a D-FF structure relative to that of α1. A positive value implies lower ring stability or higher ring strain than α1. The large positive ΔE_R for the GG conformers of the C1−O1 chain (e.g., α4a, α4b, β4*, and β5*) is a manifestation of steric congestion and/or strong H-bonds that stress the ring. The small negative ΔE_R for the βi conformers (e.g., β1−β9) suggests that the β ring is inherently more stable than the α ring, possibly because of a greater separation of the two hydroxymethyl chains.

The H-Bonds. The H-bonds O−H···O and their nonbonded distances H···O are listed in Table 3. (*iHk* is an abbreviation for O*i*−H*j*···O*k*.) The cutoff distance for H···O is 2.6 Å, the sum of van der Waals radii for the H (1.2 Å) and O (1.4 Å) atoms. All listed bonds satisfy the criteria that the O−H···O angle be greater than 90° and the donor and acceptor oxygen atoms be separated by at least two carbon atoms.[36] The shortest H···O is around 1.9 Å for 3*H*6, a transannular interaction with three ring atoms separating the two oxygen atoms. Most H-bonds are 2-center type (with one acceptor atom), but there are some 3-center type (with two acceptor atoms) in the GG conformation of the C6−O6 chain (e.g., O6−H vs O5 and O2 in β1 of Figure 1).

Two groups of conformers, α1−α9 and β1−β9, are used to relate hydrogen bonding to relative stability. The structures in Figures 3 and 4 show clearly that all αi share the same ring shape with C3 up and all βi share the same ring shape with C3 down. In synchronization with the ring shape, αi have either 4*H*2 or 2*H*4 and all βi have 3*H*2 and a g+G−g− conformation of the H−O4−C4−C3−O3−H fragment. (In 1,2-ethanediol there are 10 distinct conformations, among which g+G−g− is the second most stable.[37,38]) Anomeric stabilization is in full operation for most structures (d2 = g+ or g−) but reduced for α7, β7, β8, and β9 (d2 = t). The αi conformation related to d2 = g− is stabilized by the H-bond 2*H*4 in D-FF, whereas it is unstable in 2-HO-THF because of the steric repulsion O2−H···H−C4. There are other examples of unstable 2-HO-THF conformations turning stable in the D-FF environment owing to hydrogen bonding.

The nine distinct hydroxymethyl conformers are laid out in 3-by-3 arrays, showing variations of the C6−O6 chain (X6) from GG, GT, to TG in each column and the C1−O1 chain (X1) from GT, GG, to TG in each row. First consider the columns. Calculations indicate that regardless of the X1 orientation, relative stability of the X6 orientation is GG > GT > TG. This means α1 > α2 > α3, ..., β7 > β8 > β9: conformers decrease in stability from top to bottom. The trend is the consequence of two geometric factors: (a) the presence of 6*H*5 in GG and GT but not TG making GG, GT > TG, and (b) the participation of O6−H in GG to form transannular bonding such as 3*H*6, 6*H*1, or 6*H*2 making GG > GT, TG. Next consider the rows where the X6 orientation remains the same while X1 varies. The relative stability as a result of X1 orientation appears less systematic. Proximity of O1−H to O5, O2−H, and O3−H creates a web of H-bonds (1*H*5, 1*H*3 or 3*H*1, and 2*H*1 or 1*H*2) and lone pairs that defies simple categorization.

The limited number of α* and β* structures in Figure 5 are used as examples to identify the features that distinguish the two major ring shapes in each anomer. What seems to propel a C3-up α to a C4-up α* ring shape is the breakup of the H-bond between O2 and O4, e.g., 4*H*2 or 2*H*4 exists in α4 and α8 but is absent in α4* and α8*. Note that α8 is 2.57 kcal/mol more stable than α8* although both have the same exocyclic conformation; this energy difference is comparable to the 2.99 kcal/mol difference between 2-HO-THF αg and αg*. There seems to be no uniform mechanism to switch a C3-down β to a C4-down β* ring shape. The change requires a transformation of gauche O4−C4−C3−O3 in βi to its trans form in βi*.

The H-bond networks in the low-energy conformers with the α and β ring shapes follow some characteristic patterns. Two patterns are highlighted by replacing α1 by α1a and β7 by β7a. The resulting column (α1a, α2, α3) exhibits a favorite pattern for the GT conformation of the C1−O1 chain on the right. Likewise, the row (β1, β4, β7a) shows a favorite pattern for the GG conformation of the C6−O6 chain on the left. Favorite patterns for other hydroxymethyl conformations may be identified by examining structures listed in Table S1.

A pattern consisting of a 3-H-bond loop in a counterclockwise (CCW) or clockwise (CW) direction brings great stability to GGGG conformers α4, α4a, α4b, and β4*. Note α4 and α4a

have H atoms linking O1, O3, and O6 in a CCW loop (1*H*3, 3*H*6, and 6*H*1); the loop is reversed to CW in α4b. A similar CCW loop pattern is identified in *β*4* with O2 taking the place of O1 in α (2*H*3, 3*H*6, and 6*H*2). Each upper loop is reinforced by an H-bond below the ring linking O2 and O4 in α*i* (4*H*2 or 2*H*4) and O1 and O4 in *βi** (4*H*1). A CCW hydrogen loop in *β*7, *β*8, and *β*9 on the right side of the ring that links O1, O3, and O2 is also noted.

The H-bond strength may be estimated by choosing an appropriate pair of conformers and matching their energy difference to the difference in their H-bonds. This approach is consistent with the observation made by Ma et al.[18] in their study of gaseous hexoses. In view of the very narrow energy ranges for ΔE_e in Table 1 and the large number of different *iHk* shown in Table 3, the task of determining the influence of individual *iHk* on stability becomes formidable. Inequities in anomeric stabilization, steric and electrostatic repulsions, and ring strain further complicate the analysis. Nonetheless, we have come to some rough estimates for their relative strength as shown in Appendix S.

The transannular H-bonds 3*H*6, 6*H*3, 6*H*2, 4*H*2, and 2*H*4 occurring in the most stable structures such as α1, α4, α1a, α4a, α4b, and *β*1 and the analogous 3*H*6 and 4*H*1 in *β*4* are found to be the strongest. The estimated high and low H-bond energies are 2.6 kcal/mol for 3*H*6 and 0.6 kcal/mol for 6*H*5, which may be compared with the electron-diffraction value of 1.4 kcal/mol found in 1,2 ethanediol (cf. 2*H*1).[38] Generally the O−H···O bond strength depends on the geometry and charges of the three atoms. A shorter H···O and larger atomic charges usually lead to a stronger H-bond. The approximate ranking of the different H-bond strength in Appendix S appears consistent with this implication. The net H-bond energy in D-FF is expected to be smaller than the anomeric stabilization energy, which is the reason that the ring shapes of 2-HO-THF are mostly preserved. Moreover, the intramolecular H-bonds are generally weaker than the intermolecular H-bonds formed in aqueous solution and in solid polysaccharides (vide infra).

Ring Conformations. To gain an understanding of the influence of substituents on anomeric effect and the resulting ring shape, we list relevant geometric parameters of α3, α7, α4a*, *β*2, *β*7, and *β*5* in Table 4 for one-on-one comparisons with the six model structures αg, αt, αg*, *β*g, *β*t, and *β*g* from 2-HO-THF. The selected D-FF structures have physical features fairly close to the model structures and thereby help identify the few discrepancies. Note that the bond lengths involving the anomeric C2 follow the established trends C2−O5 ≈ C2−O2 for α3 and *β*2 where endo-AS and exo-AS coexist, C2−O5 < C2−O2 for α7 and *β*7 with only endo-AS, and C2−O5 > C2−O2 for α4a* and *β*5* with only exo-AS. As for the ring shapes, the D-FF phase angles are within 8° of the corresponding 2-HO-THF values. The puckering parameter *q* is within ±0.02 of the model values for α*i* and *βi* but is significantly smaller for α4a* and *β*5* as a consequence of strengthening certain H-bonds.

Overall, the comparison shows a reasonable agreement between each selected D-FF structure vs its 2-HO-THF counterpart. Even in α1 and *β*1, where strong H-bonds exist, the relevant geometric parameters (Table S2) can be recognized as offspring of αg and *β*g. We therefore conclude that the substituents in D-FF do not exert enough influence to alter the major ring features originated from 2-HO-THF.

Atomic Partial Charges. The dipole moment μ of each structure is related to its overall charge distribution. Unlike 2-HO-THF, simple correlations between conformations and μ are hard to find for D-FF because of the added substituents (Table 4). The CHELPG charges[26] (e) in each structure depict a point charge distribution that approximates the calculated μ reasonably well. Charges on O*i* and H*j* bonded to O*i*, H*j* (O*i*), may be related to the relative basicity and acidity at the respective oxygen and hydrogen sites and are important to the study of carbohydrate chemistry and mass spectrometric analyses on biochemical molecules.[21] In molecular modeling the calculated charges are used for evaluating electrostatic interactions.[20]

Ranges of the CHELPG charges from the six α*i* and *βi* of Tables 4 (α3, α7, *β*2, and *β*7) and S2 (α1 and *β*1) are O5 [−0.47, −0.58]; O1 [−0.68, −0.72]; O6 [−0.63, −0.72]; O3 [−0.69, −0.74]; O4 [−0.72, −0.77]; O2 [−0.66, −0.76]; and H*j* (O*i*) [0.39, 0.49]. These D-FF charges are compatible with the charges of reference compounds represented by dimethyl ether, ethanol, 2-propanol, *tert*-butyl alcohol, 1,2-ethanediol, THF, and 2-HO-THF (Table 4 footnote b).

We observe three major conditions that cause a D-FF charge to become noticeably lower than the reference value. (The term "low" or "high" implies a smaller or a larger magnitude, respectively.) The first condition is the presence of the H-bond O*i*-H*j*···O*k*, *iHk*, which decreases the negative charge on O*k*. This is the same as saying that a H-bond decreases the basicity of the proton acceptor. When the interaction is strong, the charges of all three atoms may be reduced. An example is the strong 3*H*6 in α7 which results in smaller negative charges on O6 (−0.63) and O3 (−0.69) and smaller positive charge on H10 (0.39) compared with those on the same three atoms in most other structures. Another example is the low O1 charge (−0.66) in *β*5* because of the strong 4*H*1. For most D-FF structures, the O6 and O4 atoms rarely are proton acceptors and their charges usually are quite predictable.

The second condition arises from anomeric interaction between O5 and O2 which reduces the O2 charge when the O2−H9 bond is switched from a gauche to a trans orientation against C2−O5 (i.e., from d2 g+ to t). One example is a change of O2 charge in 2-HO-THF from αg −0.73 to αt −0.66, which is replicated by D-FF from α3 −0.76 to α7 −0.66. The influence of anomeric interaction on the O2 and O5 charges, however, is often tempered by hydrogen bonding. An example of multiple interactions influencing the charge is O2 of *β*2: O2 is anomeric with O5 (d2 g−), a proton donor to O1 (2*H*1), and a proton acceptor from both O3 and O6 (3*H*2 and 6*H*2). The O2 charge of *β*2 is −0.67, on the low side, inferring that hydrogen bonding in this structure is more influential than anomeric effect. Generally, the O2 charge in a D-FF structure is the least predictable because of the many OH groups in close proximity.

The third condition is the gauche oxygen interaction in an O−C−C−O fragment that reduces the oxygen charges with or without hydrogen bonding. From separate calculations we found that the lower and higher O*i* charges in 1,2-ethanediol are associated with the gauche and trans O···O interactions, respectively. In D-FF, the O5 charges in *β*1 (−0.47) are low in part because of the gauche orientations of O5 vs O1 and O5 vs O6 plus the two weak H-bonds 1*H*5 and 6*H*5. (The same situation occurs in *β*2 and *β*5*.) Then, there is *β*5b with a low O5 charge (−0.51) where the two gauche O···O pairs are present without H-bonds. These charges are clearly different from the high O5 charge (−0.70) in *β*9 where the two O···O pairs are present in the trans orientations without forming H-bonds with O5. In a D-FF structure, all six oxygen atoms are part of one or more O−C−C−O networks, which makes the charge analysis quite difficult.

In the CHELPG framework the lower charges may imply that intramolecular interactions have tied up a certain amount

of charges to increase stability at the expense of reducing reactivity. Two D-FF structures that have high stability as a result of significant internal interactions are α1 and β1. In view of this situation, the higher oxygen charges from the given ranges are taken to represent charges free of internal interactions:

O*i*	O5	O1	O6	O3	O4	O2
charge	−0.58	−0.72	−0.72	−0.74	−0.77	−0.76
β5b	−0.51	−0.73	−0.70	−0.76	−0.77	−0.73

These O*i* charges are consistent with the trend set by simple ethers and alcohols: O5 (ether) < O1, O6 (primary alcohol) < O3, O4 (secondary alcohol) ∼ O2 ("tertiary" alcohol). Thus, it is likely that O2 is the most basic and O5 is the least basic. Experiments indeed confirm that O2 is likely the most active site for reactions. One D-FF structure expected to follow the "free" O*i* charges is β5b, which has no H-bond. The fact that fructose residues in solid polysaccharides have intermolecular instead of intraresidue H-bonds suggests that an absence of the latter leads to higher oxygen charges and stronger interactions with other species in the medium.

Comparison with Experiments. There is a serious lack of structural data on monomeric D-FF because of tautomerism. Consequently, the calculated geometries for isolated D-FF (or D-FF in the gas phase) have to be checked against the crystal data of fructose-containing polysaccharides, despite the incompatibility in physical state and composition.

Mean values of selected geometrical parameters were calculated from the HF/6-31G* values for α1−α9 and β1−β9. Results are shown in Table 5 for the α and β anomers separately. Mean values for the two anomers are quite similar, agreeing to within 0.01 Å for bond length and 1° for bond angles. However, β has lower mean absolute deviations than α owing to a greater regularity in geometry and hydrogen bonding. To gain some perspective on the accuracy of HF/6-31G* geometries, mean values of β*i* are compared to the neutron diffraction values for the fructose residue of sucrose.[10] Excluding those affected by chemical bonding between the two residues of sucrose at the anomeric carbon atom (C5−O5, C2−O5, and C2−O2), differences in bond length are 0.00−0.01 Å for C−H and C−C and 0.01 Å − 0.02 Å for O−H and C−O. Bond angles associated with the ring agree to 1°. These data confirm that HF/6-31G* yields reasonable results for parameters involving the C and H atoms but shorter bond lengths for the highly electronegative O atom.[21,23] After we include electron correlation in the optimizations for α1 and β1 (vide infra), the O−H and C−O bond lengths are increased by 0.02−0.03 Å on going from HF/6-31G* to MP2/6-31G* and MP2/6-31+G**.

Owing to the existence of a minimal intramolecular but maximal intermolecular hydrogen bonding in crystalline sugars, it is difficult to find a calculated structure for the gas phase that matches the measured geometry of a fructose residue in the solid phase. The ideal way is to obtain the calculated structure from geometry optimization in the crystal environment.[5a,15] Our approach is to find the structure of a free molecule with a conformation closest to the solid structure. After numerous attempts, we obtained for comparison in Table 5 α8* with the α* GTTG residue 1 of di-D-FF anhydride III (A1),[8] β8a* and β5 with the β* GTTG residue 1 (K1) and β GTGG residue 2 of 1-kestose (K2),[9] and β7a with the β GGTG residue of sucrose (SF).[10] The objective is to find how well the calculated ring conformations fare against the X-ray and neutron diffraction values for the α*, β*, and β forms. Lacking for comparison is the α form which has not been observed.

In each solid fructose residue,[8−10] nearly all H-bonds are intermolecular, with the majority of hydroxyls functioning as both donor and acceptor groups. (Sucrose has two interresidue bonds.) In each free molecule, there are internal H-bonds even though the structure has the same hydroxymethyl conformation and roughly the same ring shape as its solid partner. In view of the different physical forces that exist in the solid and gas samples, we do not expect good and consistent agreements between the calculated and experimental ring parameter values. On the basis of the dihedral angles φi and phase angle φ in Table 5, the match is poor for A1 ($^4T_3$) vs α8* (^4_5T), good for K1 ($_4T^3$) vs β8a* ($_4T^5$) and SF ($_3T^4$) vs β7a ($^4T_3$), and excellent for K2 ($_3E$) vs β5 ($_3E$). Nonetheless, the good agreement in two pairs of β*i* (K2 vs β5 and SF vs β7a) and the fact that many solid fructose residues are in the β form[12] suggest that it is practical to use HF/6-31G* for predicting fructose structures.

Recently, a molecular dynamics study on α,α-trehalose showed that sugars exhibit water-structuring characteristics in hydration.[39] In the context of this work, the calculated structural details of a D-FF molecule (e.g., β5) are important because they can be used to project how the structure interacts with solvent. The calculated dipole moment also provides useful information with regard to how favorably the structure interacts with polar solvents. On the other hand, hydration disrupts intramolecular H-bonds to form stronger intermolecular H-bonds and causes significant changes in the conformation and charge distribution of the solute. Several recent quantum mechanical investigations on carbohydrates include the solution effects.[5,18,33]

Basis Set (BS) and Electron Correlation (EC). A theoretical level L is expressed as M/B where M is the method and B is the basis. The overall level L2//L1 indicates that energy is calculated at L2 and geometry is optimized at L1. In the case of a large molecule for which a high-level L2 becomes impractical, an approximation may be made by the composite level "L2". The idea is to obtain the E_e of a higher correlation method and larger BS at a lower cost.[22a] To find the best practical level to calculate relative energy, as measured by the ΔE_e of 2-HO-THF αg* relative to αg or D-FF β1 relative to α1, L2//L1 is raised systematically in Table 6. The goal is to find how ΔE_e depends on the BS and EC and to deduce the lowest level at which ΔE_e converges.

The ΔE_e of αg* appears to be relatively inert to changes in BS and EC. At the HF/6-31G* geometry, successive basis extensions 6-31G* → 6-31+G** → 6-311++G** have virtually no effect on ΔE_e, showing that the 6-31G* basis is adequate. The ΔE_e values calculated at the HF/6-31G* level, with geometry improved from HF/6-31G*, MP2/6-31G*, to MP2/6-31+G**, appear nearly constant, indicating that the HF/6-31G* geometry is reasonable. At the MP2/6-31G* geometry, inclusion of correlation HF → MP2 increases ΔE_e by 0.55 kcal/mol and an upgrade MP2 → MP4 induces a small decrease of 0.22 kcal/mol; these data suggest that MP2 has slightly overcorrected HF and MP4 may be unnecessary. Similar changes of ΔE_e are seen for HF → MP2 → MP4 at the MP2/6-31+G** geometry. From these considerations, we deduce that conformational properties of 2-HO-THF may be calculated at the MP2/6-31G*//HF/6-31G* level with sufficient accuracy.

The ΔE_e of αg* reflects differences in anomeric stabilization (ΔE_{AS}) and ring strain (ΔE_R) of an equatorial (αg*) relative to an axial (αg) conformer of a furanose ring, i.e., $\Delta E_e = \Delta E_{AS} + \Delta E_R$. The term ΔE_R has been shown as −0.16 kcal/mol at the HF/6-31G* optimized level and may be taken as constant (Appendix S). The ΔE_{AS} is expected to be positive because αg possesses a greater AS (with both exo and endo) than αg* (with endo only). The calculated change of ΔE_{AS} of 0.69 kcal/mol

(0.53 + 0.16) on going from the HF/6-31G* to MP2/6-31G* optimized levels implies that correlation enhances anomeric effects.

For the pyranose ring, effects of BS and EC on the conformational energies of 2-methoxytetrahydropyran (2-MeO-THP) were examined previously.[40] The ΔE_e of the equatorial (EGT) relative to the axial (AGT) conformation was found to decrease by 0.53 kcal/mol for 6-31G* → 6-311++G** at the HF/6-31G* geometry and increase by 0.76 kcal/mol for HF → MP2 on going from the HF/6-31G* to MP2/6-31G* geometries (Table 2 of ref 40). Our separate calculations on 2-HO-THP (Table S7) give the respective decrease of 0.54 and increase of 0.41 kcal/mol; the latter compares well with an increase of 0.53 kcal/mol for the 2-HO-THF αg* vs αg (Table 6). The insignificant decrease of 0.06 kcal/mol for MP2 → MP4 at the MP2/6-31G* geometry for 2-HO-THP (Table S7) confirms once again that MP4 is unnecessary.

The ΔE_e of β1 varies dramatically with changes in EC and BS. After the Mulliken overlap populations[23] for the H···O region of all relevant H-bonds in α1 and β1 were analyzed, the very strong H-bond 3*H*6 in α1 is identified as the main cause of this variation. The H-bond distance r(3*H*6) is next used to monitor ΔE_e. Note that ΔE_e decreases as the basis extends, e.g., 0.18 → −0.94 → −1.26 kcal/mol as 6-31G* → 6-31+G** → 6-311++G** in HF optimizations, accompanied by an increase of r(3*H*6) 2.05 → 2.10 Å → 2.13 Å. Note also that ΔE_e increases as correlation is included in optimizations, e.g., 0.18 → 2.67 as HF → MP2 with the 6-31G* basis, accompanied by a decrease of r(3*H*6) 2.05 → 1.91 Å. These observations indicate that basis extension weakens, while electron correlation strengthens, hydrogen bonding. We omit the MP4 correction because of its high cost and generally insignificant impact on the MP2 conformational energies (vide supra).[22b]

The three highest optimization levels MP2/6-31G* (*l*), MP2/6-31G** (*m*), and MP2/6-31+G** (*n*) yield 2.67, 2.44, and 0.96 kcal/mol for ΔE_e, respectively. In search of a limit for ΔE_e convergence at the MP2 level, we formulate the composite level "MP2/6-311++G**" //MP2/6-31+G** (*z*) which yields 0.79 kcal/mol. [Note: $\Delta E_e(z) = \Delta E_e(n) + \Delta E_e(p) - \Delta E_e(o)$ from Table 6.] Levels *l*, *m*, *n*, and *z* now exhibit a trend for convergence as the basis extends. The best or "limiting" ΔE_e is next taken as 0.79 kcal/mol for the GGGT lowest energy conformer of β-D-FF relative to that of α-D-FF. Comparison may be made to the difference of 0.9 kcal/mol for the corresponding GG conformers of β- vs α-D-GP at the "CCSD/cc-p^{T}VDZ"//MP2/cc-pVDZ level calculated by Barrows et al.[5b] (cf. **8** vs **5** of Table 1 in ref 5b).

In the subsequent D-FF calculations shown in Table 7, the composite level "MP2/6-311++G**"//HF/6-31G** (*y*) is adopted for two reasons. First, it is impractical to compute the MP2/6-31+G** geometries required by level *z* when a substantial number of structures are involved. Second, level *y* is acceptable by virtue of the small difference (0.37 kcal/mol) in the ΔE_e of β1 from the "limiting" value of level *z*. The components of level *y* are HF/6-31G** (*i*), HF/6-311++G** (*j*), and MP2/6-31G** (*k*) and their ΔE_e values are shown for discussion. [Note: $\Delta E_e(y) = \Delta E_e(k) + \Delta E_e(j) - \Delta E_e(i)$.] Again, the calculated data indicate that basis extension ($i \rightarrow j$) decreases and electron correlation ($i \rightarrow k$) increases the relative stability of structures with stronger H-bonds than α1 (e.g., α4, α4a, α4b, and β4*), whereas the effects are exactly reversed for those with weaker H-bonds than α1 (e.g., β1, β2, β3, and β7).

Our results may be compared with those of Ma et al.[18] on seven fructofuranose structures optimized at the HF/6-31G** and B3LYP/6-31G** levels in two GGGG, one GTGG, two GGGT, one GGTG, and one TGGT conformations. After examining the differences in hydrogen bonding between our lowest energy hydroxymethyl structures for the corresponding conformations (α4, α5, α1, β7, β1, β4, and β3 vs structures e−k in Figure 2 of ref 18), we conclude that our structures have lower energies. (The HF/6-31G** energies for α1, α4, β1, β3, and β7 in Table 7 are 6.84, 3.02, 4.85, 1.76, and 2.41 kcal/mol lower than those for *g*, *e*, *i*, *k*, and *h* in Table 2 of ref 18, respectively.) We abandoned the (DFT) B3LYP/6-31G* optimizations on α1 and β1 because of convergence problems. We found E_e oscillating around −687.1562271 (α1) and −687.1542025 (β1) hartrees, from which ΔE_b (β1) is estimated as 1.27 kcal/mol. Ma et al.[18] also did not report the B3LYP/6-31G** energies for these two GGGT anomers.

Equilibrium Distribution. Eleven D-FF structures of the lowest ΔE_e in Table 1 are used to evaluate equilibrium distributions at room conditions in Table 7. All relevant E_e, E_{ZP}, $E - E_0$, S, and G_{therm} are shown in Table S6. The equilibrium population pop is estimated from the Gibbs free energy ΔG. [Note: pop = 100% ($\exp_i/\Sigma_i \exp_i$), where exp = exp[$-\Delta G/(RT)$], $\Delta G = \Delta E_e + \Delta G_{therm}$, and $G_{therm} = E_{ZP} + (E - E_0) + RT - TS$.] The "MP2/6-311++G**"//HF/6-31G** and HF/6-31G*//HF/6-31G* levels are used respectively to calculate ΔE_e at 0 K and ΔG_{therm} at 298.15 K. The stability lists determined by ΔE_e and ΔG_{therm} are Electronic: α4 > β4* > α1 > α4a > α4b > β1 > α1a > α7 > β2 > β7 > β3, and Nuclear: β2 > β3 > β1 > β7 > α1a > α7 > α1 > α4b > β4* > α4 > α4a.

High electronic stability in D-FF is generally the consequence of full anomeric stabilization and strong hydrogen bonding. For the structures on the list, eight have full AS while α7, β7, and β4* have partial AS. The number of H-bonds is six for β4*, five for the other six leading structures, and four for the last four. The top five, α4−α4b, possess the strong H-bond 3*H*6. Factors favoring nuclear stability are exactly the opposite. Full AS increases the C2−O5 and C2−O2 bond-stretch frequencies and strong H-bonds increase the associated O−H torsional and bending frequencies; these effects increase ΔG_{therm} as a result of larger zero-point energy and lower entropy. Thus, the structures high on the electronic list are low on the nuclear list. Moreover, all βi have lower ΔG_{therm} than α*i*, which may be attributed to a greater separation of the two hydroxymethyl chains in βi leading to smaller steric repulsion and higher entropy. Adding ΔE_e to ΔG_{therm} yields ΔG and the following stability ranking: Overall: β1 > α1 > α4 > β4* > α1a > β2 > α4b > α4a, α7 > β7 > β3.

The most populated structures are β1 and α1 with about 30% each. The next three are α4, β4*, and α1*a* with about 10% each. The last six have small or negligible populations.

The populations calculated at the present theoretical levels show that α- and β-D-fructofuranose prefer the α and β forms (in the respective S and N ring conformations) to the α* and β* forms (in the respective N and S ring conformations). The deductions are in general agreement with those drawn from NMR studies on methyl α- and β-D-fructofuranoside[41] and MM3 modeling of fructose ring shapes,[15] except for the absence of α* form in the theoretical equilibrium mixture (Tables 7 and S8). From the results of Table 6 (ΔE_e of β1 relative to α1 at levels *l*, *m*, *n*, *y*, and *z*) one may speculate that geometry optimizations at the MP2 correlated level with a basis 6-31+G** or larger could reduce the influence of certain strong H-bonds (3*H*6 in α4, β4*, etc.) sufficiently to bring in a notable population of the α* conformers (α4*, etc.).

Concluding Remarks

The focus of this ab initio study is to show how the relative stability of D-FF structures is influenced by steric repulsion, anomeric effect, and hydrogen bonding and to assess the calculated properties with reference to chemical experience and experimental data. In addition, a logical framework for the analysis of D-FF structures is laid out and theoretical techniques useful for the study of carbohydrates are demonstrated.

We have shown that the primary driving forces for the two general ring shapes of each D-FF anomer (α,α* and β,β*) are ring strain as in THF and anomeric stabilization as in 2-HO-THF. Internal H-bonds are chiefly responsible for the variations of charge distribution and electronic energy in α- and β-D-FF conformers. There is strong evidence that the calculated D-FF structures are sufficiently reliable to serve as model structures in future studies of sugars.

Acknowledgment. The computational support of the Ohio Supercomputer Center and the Miami Computing and Information Services, and the financial support of a National Institute of General Medical Sciences Grant (R15-GM52670-01) are gratefully acknowledged. We thank Mr. T. David Power for assistance on the Silicon Graphics Power Indigo (SGI) workstation purchased by a National Science Foundation Grant (DUE−9551091).

Supporting Information Available: Electronic energies of 44 α- and 28 β-D-FF structures at the HF/6-31G* optimized level in Table S1; atomic partial charges and internal coordinates for the D-FF α1 and β1 anomers at the HF/6-31G* optimized level in Table S2; electronic energy, dipole moment, atomic partial charges, and geometrical parameters for THF and 2-HO-THF (t, g*, and g) at different optimized levels in Tables S3 and S4; ring conformations in THF, 2-HO-THF, and D-FF at the HF/6-31G* optimized level and comparison with experiments in Table S5; electronic energies and thermodynamic properties for low-energy D-FF structures at different theoretical levels in Table S6; electronic energies for the 2-HO-THP AGT and BGT conformations at different levels in Table S7; NMR $^3J_{HH}$ coupling constants for the D-FF α1, α4*, β1, and β4* structures at the HF/6-31G** optimized level in Table S8; HF/6-31G* structures for the D-FF β5b and β7a conformers in Figure S; and procedures for estimating ring energy and H-bond energy in Appendix S. This information is available free of charge via the Internet at http://pubs.acs.org.

References and Notes

(1) Shallenberger, R. S. *Advanced Sugar Chemistry*; AVI: Westport, 1982.

(2) Saenger, W. *Principles of Nucleic Acid Structure*; Springer-Verlag: New York, 1984.

(3) Colins, P.; Ferrier, R. *Monosaccharides: Their Chemistry and Their Roles in Natural Products*; Wiley: New York, 1995.

(4) Polavarapu, P. J.; Ewig, C. S. *J. Comput. Chem.* **1992**, 13, 1255.

(5) (a) Barrows, S. E.; Dulles, F. J.; Cramer, C. J.; French, A. D.; Truhlar, D. G. *Carbohydr. Res.* **1995**, 276, 219. (b) Barrows, S. E.; Storer, J. W.; Cramer, C. J.; French, A. D.; Truhlar, D. G. *J. Comput. Chem.* **1998**, *19*, 1111.

(6) Takagi, S.; Jeffrey, G. A. *Acta Crystallogr.* **1977**, *B33*, 3510.

(7) (a) Dais, P.; Perlin, A. *Carbohydr. Res.* **1985**, *136*, 215. (b) Dais, P.; Perlin, A. *Carbohydr. Res.* **1987**, *169*, 159.

(8) (a) Taniguchi, T.; Uchiyama, T. *Carbohydr. Res.* **1982**, *107*, 255. (b) Taniguchi, T.; Sawada, M.; Tanaka, T.; Uchiyama, T. *Carbohydr. Res.* **1988**, *177*, 13.

(9) Jeffrey, G. A.; Park, Y. J. *Acta Crystallogr.* **1972**, *B28*, 257.

(10) (a) Brown, G. M.; Levy, H. A. *Acta Crystallogr.* **1973**, *B29*, 790. (b) Jonathan, C. H.; Sieker, L. C.; Jensen, L. H. *Acta Crystallogr.* **1973**, *B29*, 797.

(11) Cassady, C. J. Gas-Phase Basicities of Small Carxbohydrates; The 41st ASMS Conference on Mass Spectrometry, San Francisco, CA, May 31, 1993; private communication, 1997.

(12) French, A. D. *Carbohydr. Res.* **1988**, *176*, 17.

(13) French, A. D. *J. Plant Physiol.* **1989**, *134*, 125.

(14) French, A. D.; Tran, V. *Biopolymers* **1990**, *29*, 1599.

(15) French, A. D.; Dowd, M. K.; Reilly, P. J. *J. Mol. Struct. (THEOMCHEM)* **1997**, *395*−*396*, 271.

(16) Woods, R. J.; Szarek, W. A.; Smith, V. H., Jr. *J. Am. Chem. Soc.* **1990**, *112*, 4732.

(17) (a) Serianni, A. S.; Chipman, D. M. *J. Am. Chem. Soc.* **1987**, *109*, 5297. (b) Garret, E. C.; Serianni, A. S. In *Computer Modeling of Carbohydrate Molecules*; French, A. D.; Brady, J. W., Eds.; ACS Sympoosium Series No. 430; American Chemical Society: Washington, DC, 1990; pp 91−119. (c) Garret, E. C.; Serianni, A. S. *Carbohydr. Res.* **1990**, *206*, 183.

(18) Ma, B.; Schaefer, H. F., III.; Allinger, N. L. *J. Am. Chem. Soc.* **1998**, *120*, 3411.

(19) French, A. D.; Brady, J. W. In *Computer Modeling of Carbohydrate Molecules*; French, A. D.; Brady, J. W., Eds.; ACS Symposium Series No. 430; American Chemical Society: Washington, DC, 1990; pp. 1−19.

(20) (a) Senderowitz, H.; Parish, C.; Still, W. C. *J. Am. Chem. Soc.* **1996**, *118*, 2078. (b) Damm, W.; Frontera, A.; Tirado-Rives, J.; Jorgensen, W. L. *J. Comput. Chem.* **1997**, *18*, 1955.

(21) Jebber, K. A.; Zhang, K.; Cassady, C. J.; Chung-Phillips, A. *J. Am. Chem. Soc.* **1996**, *118*, 10515.

(22) (a) Zhang, K.; Chung-Phillips, A. *J. Phys. Chem.* **1998**, *102*, 3625. (b) Zhang, K.; Chung-Phillips, A. *J. Comput. Chem.* **1998**, *19*, 1862.

(23) Hehre, W. J.; Radom, L.; Schleyer, P. v. R.; Pople, J. A. *Ab initio Molecular Orbital Theory*; Wiley: New York, 1986.

(24) Frisch, M. J.; Trucks, G. W.; Schlegel, H. B.; Gill, P. M. W.; Johnson, B. G.; Robb, M. A.; Cheeseman, J. R.; Keith, T.; Petersson, G. A.; Montgomery. J. A.; Raghavachari, K.; Al-Laham, M. A.; Zakrzewski, V. G.; Ortiz, J. V.; Foresman, J. B.; Cioslowski, J.; Stefanov, B. B.; Nanayakkara, A.; Challacombe, M.; Peng, C. Y.; Ayala, P. Y.; Chen, W.; Wong, M. W.; Andres, J. L.; Replogle, E. S.; Gomperts, R.; Martin, R. L.; Fox, D. J.; Binkley, J. S.; Defrees, D. J.; Baker, J.; Stewart, J. J. P.; Head-Gordon, M.; Gonzalez, C.; Pople, J. A. *Gaussian 94*; Gaussian: Pittsburgh, 1994.

(25) (a) Parr, R. G.; Yang, W. *Density-Functional Theory of Atoms and Molecules*; Oxford University: New York, 1989. (b) Lee, C.; Yang, W.; Parr, R. G. *Phys. Rev. B.* **1988**, *37*, 785.

(26) Breneman, C. M.; Wiberg, K. B. *J. Comput. Chem.* **1990**, *11*, 361.

(27) Curtiss, L. A.; Raghavachari, K.; Pople, J. A. *J. Chem. Phys.* **1993**, *98*, 1293.

(28) Pople, J. A.; Scott, A. P.; Wong, M. W.; Radom, L. *Isr. J. Chem.* **1993**, *33*, 345−350.

(29) Marchessault, R. H.; Perez, S. *Biopolymers* **1979**, *18*, 2369.

(30) (a) Cremer, D.; Pople, J. A. *J. Am. Chem. Soc.* **1975**, *97*, 1358. (b) Cremer, D. *Ring*; QCPE (Indiana University): Bloomington, 1998.

(31) (a) Geise, H. J.; Adams, W. J.; Bartell, L. S. *Tetrahedron* **1969**, *25*, 3045. (b) Almenningen, A.; Seip, H. M.; Willadsen, T. *Acta Chem. Scand.* **1969**, *23*, 2748. (c) Engerholm, G. G.; Luntz, A. C.; Gwinn, W. D.; Harris, D. O. *J. Chem. Phys.* **1969**, *50*, 2446.

(32) (a) Kirby, A. J. *The Anomeric Effect and Related Stereoelectronic Effects at Oxygen*; Springer-Verlag: Berlin, 1983. (b) Juaristi, E.; Cuevas, G. *The Anomeric Effect*; CRC: Boca Raton, 1995.

(33) Cramer, C. J.; Truhlar, D. G.; French, A. D. *Carbohydr. Res.* **1997**, *298*, 1.

(34) Salzner, U.; Schleyer, P. v. R. *J. Org. Chem.* **1994**, *59*, 2138.

(35) Reed, A. E.; Curtiss, L. A.; Weinhold, F. *Chem. Rev.* **1988**, *88*, 899.

(36) Steiner, T.; Saenger, W. *Acta Crystallogr.* **1992**, *B48*, 819.

(37) Cramer, C. J.; Truhlar, D. G. *J. Am. Chem. Soc.* **1994**, *116*, 3892.

(38) Kazerouni, M. R.; Hedberg, L.; Hedberg. K. *J. Am. Chem. Soc.* **1997**, *119*, 8324.

(39) Liu, Q.; Schmidt, R. K.; Teo, B.; Karplus, P. A.; Brady, J. W. *J. Am. Chem. Soc.* **1997**, *119*, 7851.

(40) Tvaroska, I.; Carver, J. P. *J. Phys. Chem.* **1994**, *98*, 9477.

(41) Duker, J. M.; Serianni, A. S. *Carbohydr. Res.* **1993**, *249*, 281.